



Modelling and Performance Analysis of Hydrocyclones: The Case of Buzwagi Gold Mine

Alphonse Wikedzi^{1*} and Thomas Mütze²

¹University of Dar es Salaam, School of Mines and Geosciences, Department of Mining and Mineral Processing Engineering, P.O. Box 35131, Dar es Salaam, Tanzania

²Helmholtz-Zentrum Dresden-Rossendorf (HZDR), Helmholtz Institute Freiberg for Resource Technology (HIF), Chemnitz Straße 40, 09599 Freiberg, Germany

* Corresponding author, email: alpho20012001@gmail.com

Received 3 May 2022, Revised 27 Jun 2022, Accepted 29 Jun 2022, Published Jun 2022

DOI: <https://dx.doi.org/10.4314/tjs.v48i2.24>

Abstract

The performance of hydrocyclones at Buzwagi Gold Mine (BGM) was investigated in three full scale survey campaigns. Thereafter, several empirical and theoretical hydrocyclone models were used for prediction of hydrocyclone performance. The survey data revealed poor performance of the grinding circuit caused by a circulating load higher than the design. Further, the poor performance of the grinding circuit had consequences on hydrocyclones overflow particle size (i.e. a much coarser product, $x_{p,80} > 200 \mu\text{m}$) than target ($125 \mu\text{m}$). In addition, the operation indicates overloading of the hydrocyclones due to feed rates being 10–18% above the design capacity. Apart from their deficiencies, BGM hydrocyclones can be categorized as very good or excellent separators in terms of separation efficiency based on partition curves, $T(x)$. The modelling of BGM hydrocyclones revealed that Nageswararao's model can well describe and predict the operation and is recommended for future simulation and optimization of the operation. Based on the survey data, there are opportunities to improve current operation through adjustment of operating conditions like dilution of hydrocyclone feed for improved classification efficiency.

Keywords: Grinding circuit; Hydrocyclone performance; Partition curve; Hydrocyclone Modelling.

Introduction

Hydrocyclones are devices widely used in mineral processing for desliming, classification, thickening and pre-concentration (Gupta and Yan 2006, Wills and Napier-Munn 2006, Rao 2011, Wills and Finch 2016). The separation inside a hydrocyclone is based on a turbulent centrifugal sedimentation, where suspended particles are exposed to centrifugal acceleration that leads to separation from the fluid carrying them (Silva et al. 2013, Samaeili et al. 2017). Due to the turbulent flow regime, this directed movement is superimposed by mixing of fine particles.

Hydrocyclones are the standard classifiers used in wet closed grinding circuits in mineral processing plants and are chosen due to their simple design, low cost, easy operation, and low maintenance requirements. Due to their significance, many researchers have attempted to evaluate the performance of hydrocyclones through experimentation and numerical modelling (Schubert 1985, Napier-Munn and Lynch 1992, Nageswararao et al. 2004, Schubert 2010). The models try to explain and predict hydrocyclones parameters for design and optimization purposes. In nature, the models are empirical, theoretical or both. At present,

empirical models are the most applicable as they provide important relationships that describe cut size, separation efficiency, throughput, and pressure drop.

Though had been speculated by the management over their poor performance, BGM hydrocyclones had not been evaluated since plant commissioning (Wikedzi 2018). Hence, any efforts towards establishing their performance became motivating.

The aim of this study was to evaluate the performance of existing hydrocyclones in operation and demonstrate which hydrocyclone model can predict that operation. The performance was evaluated by full scale survey campaign data. Thereafter, a number of hydrocyclone models, both empirical and theoretical, were chosen and used for prediction. Finally, a suitable model for the industrial operation is recommended and used for future process performance monitoring and improvement.

This paper is an extension of the first author's PhD work at TU Bergakademie Freiberg and other previous studies which mainly covered aspects on BGM gold ore breakage and liberation characteristics, BGM gold ore components breakage characteristics and BGM grinding circuit performance assessment (Wikedzi et al. 2018, 2019, Wikedzi 2020). Although Buzwagi Gold

Mine ceased its operations by the end of 2021, this work still gives valuable contribution to other researchers.

Theoretical background

Technical classifiers separate the feed into a stream of mostly fine only and another stream of coarser particles at a defined cut size. Due to stochastic factors of particle collisions and turbulence within the separating medium, some particles of the same properties will report to both streams (Schubert 1985, Schubert and Mühle 1991, Khumalo 2007).

The efficiency of classification devices like screens and hydrocyclones is typically presented by the partition curve $T(x)$ as shown in Figure 1. Partition curve is also known as performance, Tromp or T-curve (Schubert 2003, Gupta and Yan 2006, Wills and Napier-Munn 2006). The partition curve relates the weight fraction of particles with an individual size x which report to the apex (i.e. coarse product stream), to the weight fraction of those particles in the feed. From the curve, the cut size x_T is introduced and defined as the size for which 50% of the particles in the feed report to the coarse product stream. Particles of this size have an equal chance of going either with the overflow or underflow.

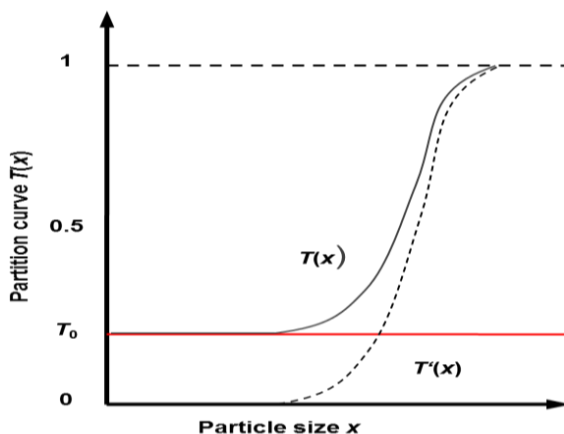


Figure 1: Typical partition curve with superimposed splitting (Mütze et al. 2019).

In most cases, $T(x)$ does not pass through the origin since a fraction of particles bypasses the separation (Gupta and Yan 2006). Thus, the processing behaviour can be

distinguished into splitting and separation. The splitting can be qualified by the split factor T_0 as highlighted in Figure 1. The cut size can be corrected to x'_T in order to

account for the bypass effect. Equations (1–5) are involved in the assessment of a given classifier (Mütze et al. 2019):

$$T(x) = (1 - R_{m,f}) \frac{\mu_c(x)}{\mu_f(x)} \quad (1)$$

Where: $R_{m,f}$ = fraction of particles recovered in the fine product
 $\mu_c(x)$ = weight fraction of particles of size x in the coarser product stream
 $\mu_f(x)$ = weight fraction of particles of size x in the feed stream

$$T'(x) = \frac{T(x) - T_0}{1 - T_0} \quad (2)$$

And

$$x'_T = T(x'_T) = 0.5 \quad (3)$$

The sharpness of the cut is represented by the slope of the central section of the partition curve; the closer to vertical is the slope, the higher is the efficiency. The imperfection (I) as well as efficiency of separation (κ) describe this feature and are being given by Equations (4) and (5):

$$I = \frac{x_{75} - x_{25}}{2x_{50}} \quad (4)$$

$$\kappa = \frac{x_{25}}{x_{75}} \quad (5)$$

x_{25} and x_{75} are sizes at which 25% and 75% of the feed particles report to the coarse stream.

Several empirical relationships (Table 1) exist for design and performance predictions of hydrocyclones. They are established from experimental investigations of hydrocyclone performances dependence on firstly; operational variables like feed pressure, feed pulp density, flow rate, etc., and secondly; on design parameters like D_c , D_i , D_o , D_a , etc. (see Figure 2).

The main hydrocyclones performance indicators estimated from such models are cut size, separation efficiency and pressure drop. This section gives an overview on such models which are widely applicable in mineral processing operations.

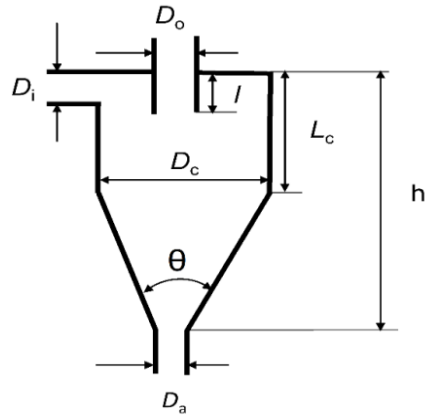


Figure 2: Hydrocyclone schematic diagram indicating design parameters. D_c : cyclone diameter, D_o : vortex finder diameter, D_i : inlet diameter, l : vortex finder length inside the cyclone, L_c : cylindrical section length, h : hydrocyclone length, θ : cone angle, D_a : apex diameter.

Plitt and co-workers (Napier-Munn et al. 1996, Nageswararao et al. 2004, Wills and Napier-Munn 2006) developed a model Equation (6) that is applicable to hydrocyclones with diameters in the range 32–150 mm and operates with dilute slurries. This model can be used to calculate the efficiency of a cyclone accurately without experimental data. Due to its mathematical nature, the parameters have to be used as non-dimensional numbers. D_c , D_a and h have to be in cm and also as defined in Figure

2. $\phi_{V,s}$ is solids content by volume, η_F is fluid viscosity (Pa.s), k is hydrodynamic exponent (i.e., $k = 0.5$ for laminar flow), and $F1$ is a material specific constant.

Another model among the well-established hydrocyclone models is an empirical model by Lynch and Rao (Napier-Munn et al. 1996, Gupta and Yan 2006), as presented in Equation (7). In the equation, \dot{V} is feed flow rate (m^3/h), $C_{w(F)}$ is the solid mass in the feed in %, Z_1 and Z_2 describe the relative amount of +420 μm and -53 μm material in the feed in %, and x_T , D_o and D_i are in cm.

Table 1: Most applicable hydrocyclone models for design and performance evaluation

Model	Equation	References
Plitt	$x_T = \frac{(F1)39.7D_c^{0.46}D_i^{0.6}D_o^{1.21}\eta_F^{0.5} \exp(0.063\phi_{v,s})}{D_a^{0.71}h^{0.38}(\dot{V})^{0.45} \left(\frac{\rho_S - \rho_F}{16}\right)^k}$	(6) (Napier-Munn et al. 1996, Nageswararao et al. 2004, Wills and Napier-Munn 2006)
Lynch & Rao	$\log x_T = 4.18D_o - 5.43D_a + 3.04D_i + 0.0319C_{w(F)} - 3.6 \dot{V} - 4.2 * 10^{-3} Z_1 + 4 * 10^{-4} Z_2$	(7) (Napier-Munn et al. 1996, Gupta and Yan 2006)
Schubert	$x_T = K \sqrt{\frac{\eta_F D_c}{(1 - \phi_{v,s})^{4.65} (\rho_S - \rho_F) \sqrt{\frac{P_A}{\rho_P}}} \ln\left(\frac{D_a}{D_o}\right)^2}$	(8) (Schubert 1985, Schubert and Mühle 1991, Schubert 2010)
Nageswararao	$\frac{x_T}{D_c} = KD_1 \left(\frac{D_o}{D_c}\right)^{0.52} \left(\frac{D_a}{D_c}\right)^{-0.47} H_S^{0.93} \left(\frac{P_A}{\rho_P g D_c}\right)^{-0.22} \left(\frac{D_i}{D_c}\right)^{-0.5} \left(\frac{L_c}{D_c}\right)^{0.2} \theta^{0.15}$	(9) (Napier-Munn et al. 1996)

An interesting model has also been set up by Schubert and co-workers (Schubert 1985, Schubert and Mühle 1991, Schubert 2010), Equation (8). This is a theoretical model based on flow characteristics (i.e., turbulent two-phase flow theory). Hence, it accounts for two flow regimes; dilute flow (< 25% solids vol. fraction) and dense flow (> 25% vol. solids fraction). Where ρ_p is the pulp density (kg/m^3), p_A the inlet pressure (bar), z an exponent expressing the flow regime and K is a material specific correction factor.

Hydrocyclones may also be modelled using an empirical relationship developed by

Nageswararao (Napier-Munn et al. 1996), Equation (9). This model was developed at JKMRRC and is an extension of the original model developed by Lynch and Rao (Equation (7)). The additional parameters in Equation (9) can be defined as follows: KD_1 is feed characteristic constant, H_s is hindered settling correction term (i.e. Equation (10)) and g is acceleration due to gravity.

$$H_s = \frac{10^{1.82\phi_{v,s}(F)}}{8.05[1 - \phi_{v,s}(F)]^2} \quad (10)$$

Furthermore, Nageswararao model is completed with more relationships as illustrated from Equation (10) to Equation (15).

$$KD_1 = KD_0 D_c^{-0.65} \quad (11)$$

$$\dot{V} = KQ_1 D_c^2 \left(\frac{P}{\rho_p}\right)^{0.5} \left(\frac{D_o}{D_c}\right)^{0.68} \left(\frac{D_i}{D_c}\right)^{0.45} \theta^{-0.1} \left(\frac{L_c}{D_c}\right)^{0.2} \quad (12)$$

For cyclones of Krebs geometry treating identical feeds:

$$KQ_1 = KQ_0 D_c^{-0.1} \quad (13)$$

$$R_f = K_{W1} \left(\frac{D_o}{D_c}\right)^{-1.19} \left(\frac{D_u}{D_c}\right)^{2.40} \left(\frac{P_A}{\rho_p g D_c}\right)^{-0.53} H_s^{2.7} \left(\frac{D_i}{D_c}\right)^{-0.5} \theta^{-0.24} \left(\frac{L_c}{D_c}\right)^{0.22} \quad (14)$$

$$R_v = K_{V1} \left(\frac{D_o}{D_c}\right)^{-0.94} \left(\frac{D_u}{D_c}\right)^{1.83} \left(\frac{P_A}{\rho_p g D_c}\right)^{-0.31} \left(\frac{D_i}{D_c}\right)^{-0.25} \theta^{-0.24} \left(\frac{L_c}{D_c}\right)^{0.22} \quad (15)$$

Where: R_v = volumetric recovery of feed slurry to underflow (%); K = fit parameter; KD_0 = calibration factor for x_T depending on feed solids characteristic; KQ_1 = calibration factor for total slurry flow rate depending on feed solids characteristic; K_{W1} = calibration factor for water recovery to underflow, and R_f = recovery of water to underflow (%).

The cut size, x_T , predicted in Equation (9) is combined with the Whiten function (Equation (16)) to determine the corrected efficiency curve for the cyclone (Napier-Munn and Lynch 1992, Reyes-Bahena 2001, Dundar et al. 2011, Ergün et al. 2005):

$$E_{oa} = C \left[\frac{(1 + \beta^* \cdot \beta^{**} \cdot Y)(\exp(\alpha_1) - 1)}{\exp(\alpha \cdot \beta^{**} \cdot Y) + \exp(\alpha_1) - 2} \right] \quad (16)$$

$$Y = \frac{x}{x_T} \quad (17)$$

Where: E_{oa} = actual efficiency expressed as the particles reporting to overflow; C = recovery of water to overflow ($1 - R_f$); a_1 = efficiency parameter; β^* = fish-hook factor; β^{**} = dummy parameter introduced to preserve the definition of x_T (i.e., $x = x_T$) when:

$$E_{oa} = \frac{C}{2} \quad (18)$$

The calibration of hydrocyclone model involves the calculation of the best fit values for α_1 , β^* , x_T and C to the plant data. If the fish-hook behaviour does not exist, then β^{**} is taken as equal to zero. The fish-hook effect (Figure 3) denotes the shape of the separation efficiency curves showing a minimum in the range of about 10 μm or

below and rising again towards finer sizes. This phenomenon originates from the hydrodynamic interaction of particles of different sizes, where fine particles are entrained by large ones for poly-dispersed suspensions (Schubert 2003). The fish-hook effect interferes with the separation efficiency of fine particles.

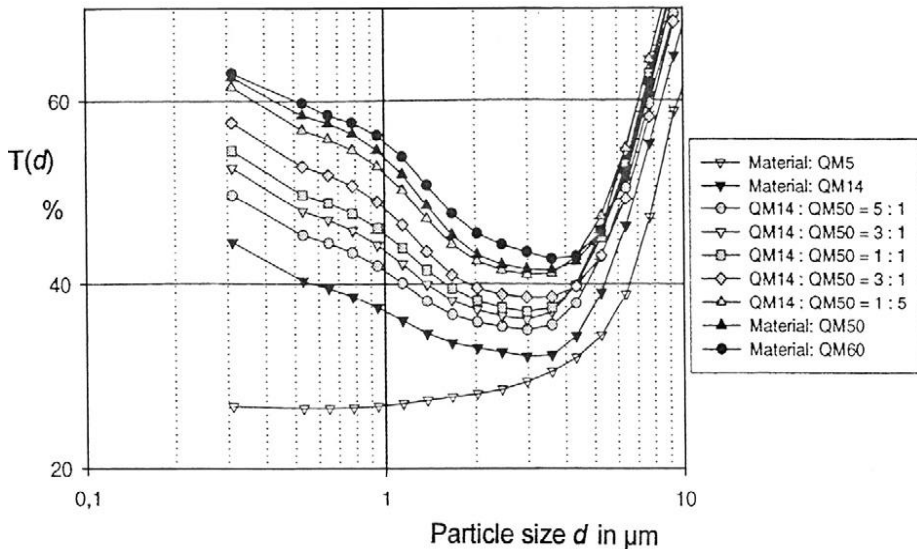


Figure 3: An example of partition curves with fish-hook behaviour obtained in a 25 mm-hydrocyclone with nine different quartzite materials (Gehart as cited in (Schubert 2010)).

Materials and Methods

Grinding circuit survey campaign

Grinding circuit survey is an essential tool for understanding the performance of the circuit over a particular time period. It involves collection of representative samples and operating data. Further, a good survey has to be conducted based on standard procedures as proposed by Napier-Munn and others (Napier-Munn et al. 1996, Mular et al. 2002).

In this investigation, data from three full scale sampling campaigns conducted between April and June 2015 (Wikedzi 2018, Wikedzi et al. 2018, 2019, 2020, Wikedzi and Leißner 2021) were used. Prior to sampling, circuit operating conditions (e.g. circuit feed rate and cyclone feed pressure) were monitored to ensure that the plant is under steady state conditions.

However, for the purpose of the present study, the crucial data were those from the secondary grinding circuit (i.e., sampling points 5–8 in Figure 4) and are the main focus in following sections. Furthermore, the samples corresponding to the three surveys are identified as S-1, S-2 and S-3 for surveys 1, 2, and 3, respectively.

Sampling of secondary grinding circuit streams

Slurry sampling for this study was done for cyclone feed, overflow, and underflow as well as the ball mill discharge. During the whole campaign, each slurry stream was sampled after every 15 minutes for a period of two hours. A total of eight subsamples were collected to make the composite weight (i.e., Table 2) for the final sample. This was done in order to reduce possible sampling

errors due to operation or process fluctuations (i.e., plant dynamics). However, the other possible sources of errors (Napier-Munn et al. 1996) could be due to sample cutter design, sub-sampling (e.g., splitting) of primary

sample, analytical errors (e.g., weighing, inadequate sieving time, etc.) as well as propagation errors due to calculation of quantities.

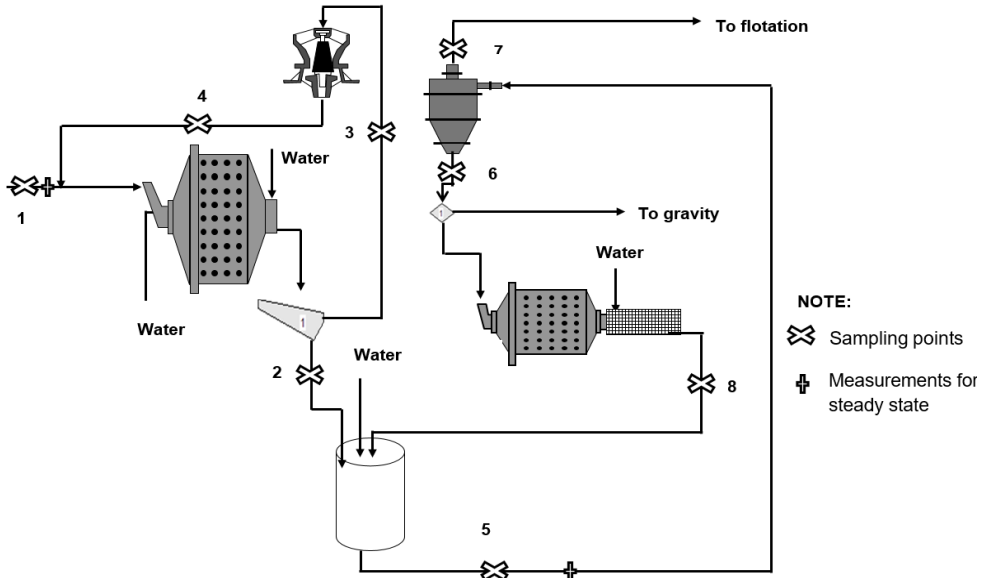


Figure 4: BGM grinding circuit flowsheet with sampling points. 1) SAG mill feed, 2) SAG mill discharge screen undersize, 3) Pebble crusher feed, 4) Pebble crusher product, 5) Cyclone feed, 6) Cyclone underflow, 7) Cyclone overflow, and 8) Ball mill discharge.

Table 2: Slurry streams composite sample weights collected

Stream/sample name	Survey		
	1	2	3
Ball mill product in kg	7.15	20.30	20.80
Cyclone feed in kg	14.22	17.66	20.83
Cyclone underflow in kg	15.60	10.40	12.50
Cyclone overflow in kg	6.60	7.80	9.90

Additional data collected

In addition to sampling, design and current operating parameters are also required. Design parameters (Table 3) were obtained from the design documents (i.e. operating manual and design criteria), while current operating parameters were obtained from the process control system and comprised of feed rate, mill power draw, mill weight, water addition rate, mill speed, cyclone pressure, etc. The ball load was determined as described in previous studies by Napier-Munn and others (Napier-Munn et al.1996, Gupta and Yan 2006).

Processing of samples

Solid’s content

All slurry samples were first filtered using a laboratory filter press and the filter cake product dried in an oven at 150 °C for a duration of 24 hours. Then, the solids content (%) was calculated using Equation (19) and details of this task are summarized in Figure 5.

$$\text{Solids (\%)} = \left(\frac{m_{\text{dry}}}{m_{\text{wet}}} \right) \cdot 100\% \tag{19}$$

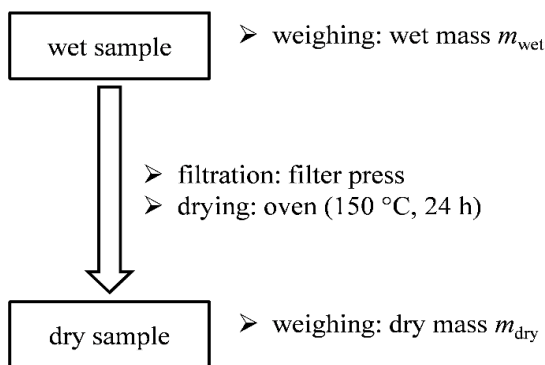


Figure 5: Procedure for solid's content determination.

Table 3: Summary of design criteria for BGM secondary grinding circuit

Design parameter	Ball mill	Hydro-cyclone
Feed rate in t/h		1500
Diameter/Length in m	6.10/9.05	
Power in kW	6000	
Ball charge in % volume	30-35	
Critical speed in %	75	
Ball size in mm	80/65/50	
Mill product $x_{p,80}$ in μm	125	
Pressure in kPa		80–110
Circulating load in %		250–350
Overflow (circuit) product $x_{f,80}$ in μm		100–125
D_c in mm		660
D_i in mm		275
D_o in mm		280
D_a in mm		150

Particle size analysis

The dried slurry samples were also used for particle size analysis. The sieving process applied for all samples is summarized in Table 4. The top sieves used depended on the expected largest particle size from the stream.

Larger top sieve (4.75 mm) was used for coarser product streams (i.e. ball mill feed, hydrocyclones feed and hydrocyclones underflow) as opposed to the finer hydrocyclone overflow product, where the top sieve of 0.425 mm was used.

Table 4: Particle size analysis procedure

Sample	Sample preparation	Sieve analysis
Hydrocyclone feed	- Splitting dried samples with riffle splitter to obtain representative subsample	- 200 mm sieves
Hydrocyclone underflow		- Sieve series in mm: 4.75, 3.35, 2.36, 1.7, 1.18, 0.85, 0.6, 0.425, 0.3, 0.212, 0.15, 0.106
Ball mill discharge		- 200 mm sieves
Hydrocyclone overflow		- Sieve series in mm: 0.425, 0.3, 0.212, 0.15, 0.106, 0.075, 0.063

Results and Discussions

This section presents the results as well as brief discussion on the modelling and performance assessment of BGM hydrocyclones operation. It provides the state of the art performance of the hydrocyclones as well as the modelling results and its implications.

Ball mill performance based on survey data

The particle size distribution of ball mill streams for the BGM operation was evaluated

and the results are presented in Figure 6. Little differences can be seen in the ball mill performance for the three surveys. As was observed in the previous studies (Wikedzi 2018, Wikedzi et al. 2019), the general conclusion is that the ball mill operation was inefficient as could not achieve target product size of 125 μm . The poor performance of the ball mill might have been due to higher circulating load and coarser feed coming from the SAG mill discharge (see Table 5).

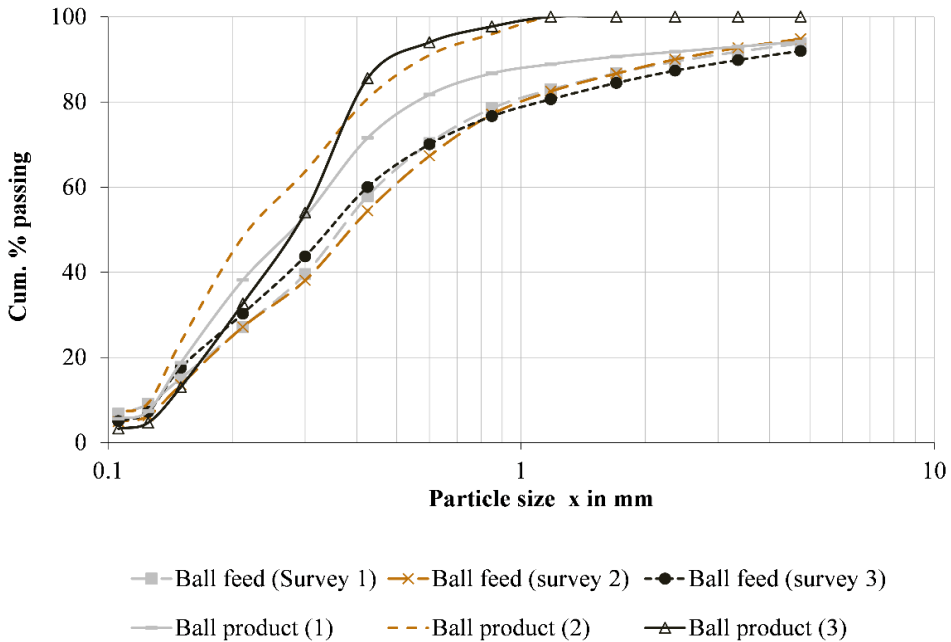


Figure 6: Ball mill feed and product size distribution for surveys 1, 2 and 3.

Table 5: Ball mill performance indicators at BGM

Parameter	Survey 1	Survey 2	Survey 3	Design/Target
Ball mill feed $x_{F,80}$ (mm)	0.963	1.028	1.127	
Ball mill discharge $x_{P,80}$ (mm)	0.570	0.419	0.403	0.125
Circulating load, CL (%)	400	344	381	250–350
Ball load, % volume	33	33	–	30–35
Ball mill specific energy (kWh/t)	4.77	5.74	10.73	14.5–16.50

Hydrocyclones performance based on survey data

Figure 7 and Table 6 present the size distributions and some key performance indicators, respectively, for the BGM

hydrocyclones as obtained during the three surveys. In all the three surveys, the results showed that the overflow (i.e. $x_{P,80}$) is much coarser than target (i.e., 125 μm).

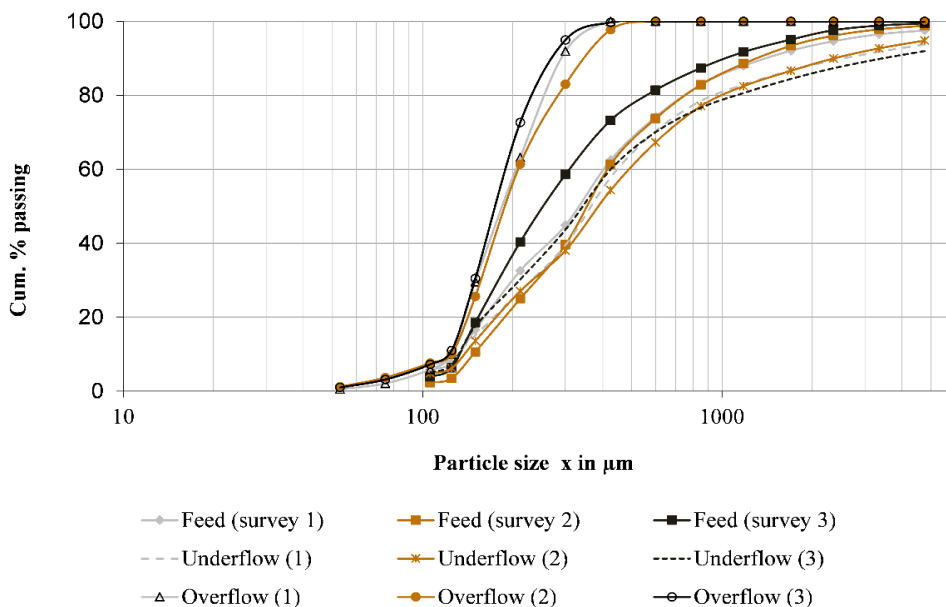


Figure 7: BGM Hydrocyclone product streams particle size distribution for the three surveys.

Table 6: Hydrocyclone performance indicators at BGM

Parameter	Survey 1	Survey 2	Survey 3	Design/Target
Feed rate (t/h)	1729	1614	1061	1500
Operating pressure (kPa)	98	81	92	80–110
Feed volume-% solids	42	44	41	33
Underflow volume-% solids	57	57	56	48–56
Overflow volume-% solids	20	24	21	13–16
Feed $x_{F,80}$ (μm)	768	771	570	
Underflow $x_{c,80}$ (μm)	963	1028	1127	
Overflow $x_{f,80}$ (μm)	266	288	241	100–125

Since the ball mill products were significantly coarser than once designed (Table 5), the coarse overflow achieved is to some degree caused by the inefficient ball mill. Also, the overflow size is influenced by hydrocyclone feed rate and feed pulp density.

The increase in feed rate to the hydrocyclone increases the centrifugal force effect which causes finer particles being carried to the underflow, and hence decreasing the cut size. Further, the sharpness of separation decreases with increasing pulp density and the separation size rises due to higher resistance to swirling motion within the cyclone which reduces the effective pressure drop (Wills and Napier-Munn 2006). In addition, feed rates for surveys 1 and 2

were 10 and 18% higher than design capacity of 1500 t/h, implying that hydrocyclones were overloaded (see Table 6). Importantly, it has to be recognized that the performance behaviour BGM grinding circuit had not been evaluated since its commissioning in 2009 (Wikedzi 2018). Hence, there are no previous data on the performance of hydrocyclones that could be incorporated with the present study.

The results of hydrocyclone efficiency for the BGM operation based on partition curve are shown in Figure 8 and Table 7. It can be observed that the by-pass fraction (split) was higher than 50% and the corrected cut size was higher than 200 μm for all the three cases. This may also be related to the coarser

overflow (i.e. $x_{P,80}$) obtained; clearly indicating that the BGM operation could not be able to achieve the target overflow size of 125 μm . The cut size and by-pass fraction are influenced by feed pulp density and feed rate (Table 6), which is in agreement with previous studies (Wills and Napier-Munn 2006, Rybinski et al. 2011). In all of the three

surveys, the hydrocyclone feed solids concentrations (%v/v) were 17 percentage higher than design (33% v/v) and also higher than what literature recommends (35% v/v) for typical operation (Wills and Napier-Munn 2006). This might have contributed to the poor separation efficiency observed.

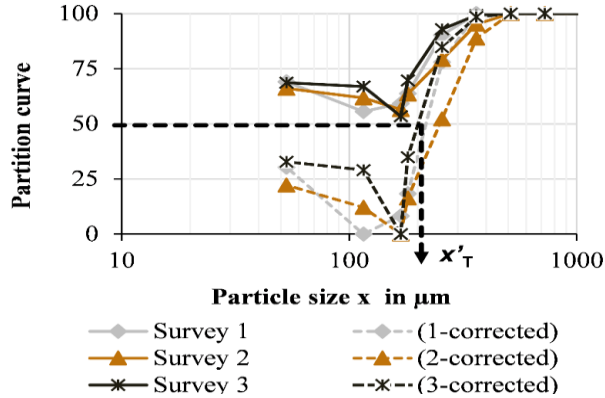


Figure 8: Uncorrected and corrected partition curves for surveys 1, 2 and 3.

Nevertheless, the corrected separation efficiency, κ , was fairly good for all surveys if the splitting effect was taken into account. Furthermore, the imperfection I (see Table 8), can be used to categorize the performance of hydrocyclones (Murthy and Basavaraj 2012). Consequently, the hydrocyclones at BGM could be categorized between very good (i.e., $0.2 < I < 0.3$) and excellent (i.e., $I < 0.2$) (see

Tables 7 and 8). This indicates that the current design is in principle fairly efficient for coarser overflow product and not for the current target (i.e., $x_{f,80} = 125 \mu\text{m}$). Preliminarily, this indicates that smaller hydrocyclones ($D_c < 660 \text{ mm}$) are required for the BGM operation to achieve the target overflow product size.

Table 7: Hydrocyclone efficiency indicators at BGM

Parameter	Survey 1	Survey 2	Survey3	Design
Split factor T_o (%)	55.60	56.00	53.42	
Corrected cut size, x_T (μm)	220.84	251.45	203.75	
Imperfection, I	0.14	0.24	0.16	
Separation efficiency, κ	0.75	0.62	0.74	
Overflow $x_{f,80}$ (μm)	266	288	241	125

Table 8: Hydrocyclone efficiency categorization based on imperfection, I

Imperfection, I - values	Separator category/classification
< 0.2	Excellent separator
$0.2 < I < 0.3$	Very good separator
$0.3 < I < 0.4$	Medium separator
$0.4 < I < 0.6$	Poor separator
$I > 0.6$	Bad separator

Hydrocyclone modelling and prediction

A suitable hydrocyclone model for prediction of BGM operation was obtained through non-linear fitting of the hydrocyclone cut sizes (i.e. from survey data) to several models reported in Table 1, by application of the SOLVER tool in Excel. This technique searches for the best combination of fitting parameters of a model by minimization of

residual errors between experimental and predicted values (Katubilwa and Moys 2009).

Table 9 summarizes the fitting results for all models and indicate that Nageswararao’s model gave close values to that from the three surveys. Therefore, this model was recommended for prediction and performance assessment of the BGM operation.

Table 9: Comparison of the cut size from hydrocyclone models fitted to survey data

Model	x_T (μm)		
	Survey 1	Survey 2	Survey 3
Survey	220.84	251.45	203.75
Plitt	246.22	298.50	306.40
Lynch and Rao	280.0	280.0	320.0
Schubert	363.80	418.60	315.60
Nageswararao	221.20	251.10	204.15

Figure 9 shows the correlation between the hydrocyclone cut sizes calculated from models with cut size values obtained from the

surveys. From the results, it can be clearly confirmed that the BGM hydrocyclones could be well explained by Nageswararao model.

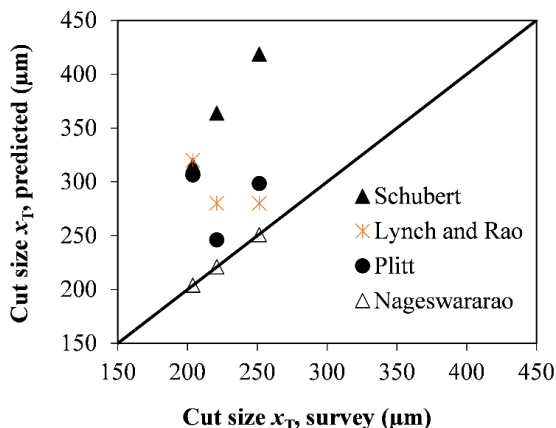


Figure 9: Correlation between model predicted and measured (survey) cut sizes, x_T for the three surveys. Lines and markers refer to predicted and survey values, respectively.

Table 10 presents several hydrocyclone models prediction capability based on residue ((difference between measured cut size and predicted one)²) as well as coefficients of

determination (R^2). Both parameters prove that Nageswararao’s model has higher predictive power for the BGM hydrocyclones operation than the other models.

Table 10: Models prediction residue and coefficients of determination

Model/Performance parameters		Survey 1	Survey 2	Survey 3
Nageswararao	Residue	8.08×10^{-12}	2.94×10^{-39}	7.35×10^{-40}
	R^2	1.00	1.00	1.00
Plitt	Residue	0.7342	0.8849	0.4325
	R^2	0.8851	0.8129	0.4962
Schubert	Residue	0.3553	0.3329	0.4541
	R^2	0.3527	0.3353	0.4510
Lynch and Rao	Residue	0.7342	0.8849	0.4325
	R^2	0.7321	0.8865	0.4294

Nageswararao’s model predictive capability based on coefficients of determination was also tested on other

hydrocyclones parameters (Figure 10) and the model could also perform well (i.e., $R^2 > 0.96$).

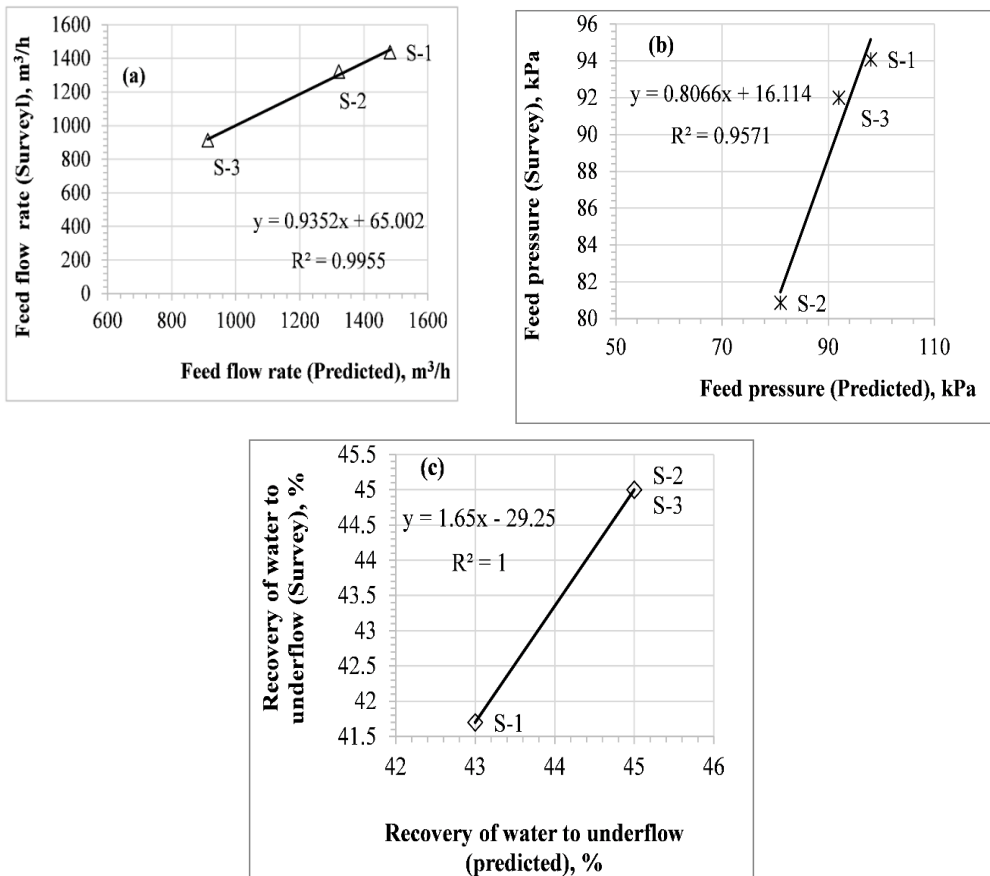


Figure 10: Nageswararao’s model prediction capability for hydrocyclones feed flow rate (a), hydrocyclones feed pressure (b) and water recovery to underflow (c). Lines and markers refer to predicted and experimental values, respectively.

Conclusions and Recommendations

The assessment of BGM grinding circuit performance based on survey data revealed poor performance of the ball mill due to the high circulating load observed. Further, the results indicate that the hydrocyclones overflow product size ($x_{P,80}$) is much coarser than target. This is caused by the poor performance of the ball mill (i.e., coarser product) as earlier identified. Moreover, hydrocyclones feed rates were up to 18% higher than design capacity, implying that the devices were overloaded. The hydrocyclone efficiency based on partition curve ranged between 0.62–0.75 which could be categorized as very good or excellent separator despite the poor product quality. This indicates that the current design is in principle fairly efficient for coarser overflow product.

The modelling of BGM hydrocyclones reveals that Nageswararao model could well describe the operation and is thus recommended for simulation and optimization of the operation. The surveys revealed several opportunities to improve BGM operation through adjustment of operating conditions. For example, the hydrocyclone feed was identified to contain high percent solids (i.e., 66.5 to 68.40%) and had also high percent solids (i.e., 41 to 47%) in the overflow. Hence, if the feed is diluted and the overflow allowed to reach a lower density, close to 30%, the classification efficiency will improve, giving a sharper cut.

Acknowledgements

The authors would like to thank Buzwagi Gold Mine (BGM) for providing the opportunity to conduct this study. The Institute of Mechanical Process Engineering and Mineral Processing, TU Bergakademie Freiberg is also acknowledged for provision of laboratory facilities and resources for the investigation.

References

Dundar H, Benzer H, Aydogan NA, Altun O, Toprak NA, Ozcan O, Eksi D and Sargin A 2011 Simulation assisted capacity improvement of cement grinding circuit:

Case study cement plant. *Miner. Eng.* 24: 205–210.

Ergün L, Gıilsoy Ö, Can M and Benzer H 2005 Optimization of Çayeli (Çbi) grinding circuit by modelling and simulation, in: *The 19th International Mining Congress and Fair of Turkey, JMCET. Izmer*, pp. 309–320.

Gupta A and Yan DS 2006 Introduction to Mineral Processing Design and Operation, Elsevier, Perth.

Katubilwa FM and Moys MH 2009 Effect of ball size distribution on milling rate. *Miner. Eng.* 22: 1283–1288.

Khumalo N 2007 *The Application of the Attainable region analysis in Comminution*. PhD thesis, University of the Witwatersrand.

Mütze T, Kretschmar G and Meer FVD 2019 Segregation of minerals in dynamic air classifiers, in: XXIX International Mineral Processing Congress (IMPC). Moscow.

Mular AL, Haibe DN and Barrett DJ 2002 Mineral Processing Plant Design, Practice, and Control, SME, Colorado.

Murthy N and Basavaraj K 2012 Assessing the performance of a floatex density separator for the recovery of iron from low-grade australian iron ore fines—a case study, in: *XXVI International Mineral Processing Congress (IMPC)*. New Delhi.

Nageswararao K, Wiseman DM and Napier-Munn TJ 2004 Two empirical hydrocyclone models revisited. *Miner. Eng.* 17: 671–687.

Napier-Munn TJ and Lynch AJ 1992 The modelling and computer simulation of mineral treatment processes—current status and future trends. *Miner. Eng.* 5: 143–167.

Napier-Munn TJ, Morrel S and Kojovic T 1996 Mineral Comminution Circuits: Their Operation and Optimization, JKMRRC, Queensland.

Rao DV 2011 Mineral Beneficiation: A Concise Basic Course, Taylor and Francis, London.

Reyes-Bahena JL 2001 Modelling and Simulation of the Grinding Circuit at

- “ELPILON” Mine, in: *JKMRC*. Brisbane, pp. 181–196.
- Rybinski E, Ghersi J, Davila F, Linares J, Valery W, Jankovic A, Valle R and Dikmen S 2011 Optimisation and continuous improvement of Antamina comminution circuit, in: *SAG Conference*. Vancouver.
- Samaeili M, Hashemi J, Sabeti M and Sharifi K 2017 Modeling and analyzing hydrocyclone performances. *Iran. J. Chem. Chem. Eng.* 36(6): 177–190.
- Schubert H 2010 Which demands should and can meet a separation model for hydrocyclone classification? *Int. J. Miner. Process.* 96: 14–26.
- Schubert H 2003 “Zu den Ursachen ‘anomaler’ Verläufe der Trennkurve bei der Feinstkornklassierung in Hydrozyklonen–insbesondere zum so genannten Fish-Hook-Effekt*.” *Aufbereit. Tech.* 44: 5–17.
- Schubert H 1985 A hydrocyclone separation model in consideration of the turbulent multi-phase flow. *Int. J. Part. Sci. Technol.* 3: 1–13.
- Schubert H and Mühle K 1991 The role of turbulence in unit operations of particle technology. *Adv. Powder Technol.* 2: 295–306.
- Silva AC, Silva EMS and Matos JDV 2013 Hydrocyclones simulation using a new modification in Plitt's equation. *IFAC Proc.* 46(16): 12–17.
- Wikedzi A 2018 *Optimization and performance of grinding circuits: The case of Buzwagi Gold Mine (BGM)*. PhD thesis, TU Bergakademie Freiberg.
- Wikedzi A 2020 Assessment of the performance of grinding circuit for Buzwagi Gold Mine. *Tanz. J. Eng. Technol.* 39: 144–164.
- Wikedzi A, Arinanda MA, Leißner T, Peuker UA and Mütze T 2018 Breakage and liberation characteristics of low grade sulphide gold ore blends. *Miner. Eng.* 115: 33–40.
- Wikedzi A and Leißner T 2021 Mineral liberation: A case study for Buzwagi Gold Mine. *Tanz. J. Sci.* 47: 892–905.
- Wikedzi A, Peuker UA, Mütze T and Shayo F 2019 Improving the grinding performance through modelling and simulation: The case of Buzwagi gold mine (BGM), in: *XXIX International Mineral Processing Congress (IMPC)*. Moscow.
- Wikedzi A, Saquran S, Leißner T, Peuker U and Mütze T 2020 Breakage characterization of gold ore components. *Miner. Eng.* 151: 106314.
- Wills B A and Finch JA 2016 *An Introduction to the Practical Aspects of Ore Treatment and Mineral Recovery*, 8th ed, Elsevier, Oxford.
- Wills BA and Napier-Munn T 2006 *Wills' Mineral Processing Technology: An Introduction to the Practical Aspects of Ore Treatment and Mineral Recovery*, 7th ed, Butterworth-Heinemann, Oxford.